crystals

MDPI

Communication

Formation of an Unusual *Pseudo*-Square Planar-Induced Mercury(II) Dimeric Complex

Huiyeong Ju [1], Dong Hee Lee [2], Seulgi Kim [3], Joon Rae Kim [4], Yunji Kang [3], Eunji Lee [4,*] and In-Hyeok Park [2,*]

[1] Western Seoul Center, Korea Basic Science Institute, Seoul 03759, Republic of Korea
[2] Graduate School of Analytical Science and Technology (GRAST), Chungnam National University, Daejeon 34134, Republic of Korea
[3] Department of Chemistry and Research Institute of Natural Sciences, Gyeongsang National University, Jinju 52828, Republic of Korea
[4] Department of Chemistry, Gangneung-Wonju National University, Gangneung 25457, Republic of Korea
* Correspondence: ejlee@gwnu.ac.kr (E.L.); ipark@cnu.ac.kr (I.-H.P.)

Abstract: Due to the different crystallization methods, two Hg(II) complexes of a 19-membered NO_2S_2-macrocycle (**L**) and its oxidized ligand (**HL$_{ox}$**), exhibiting different stoichiometries, were prepared. First, mercury(II) iodide reacts with **L** to afford a dinuclear metallacycle complex $[Hg_2(\mathbf{L})_2I_4]$ (**1**) in which the mercury(II) exists outside the macrocyclic cavity. Meanwhile, the slow diffusion reaction gave an unusual *pseudo*-square planar-induced mercury(II) complex, which shows three separated parts with the formula $[Hg_2(H\mathbf{L_{ox}})I_5]_2[HgI_2]$ (**2**). There are two complex cation units that are exo-coordinated, along with one unit consisting of a metal cluster anion. Surprisingly, **L** was oxidized in the disulfoxidized form (**HL$_{ox}$**) in this condition. NMR titration was used to monitor both the structural and binding characteristics of the complex formed between **L** and mercury(II) iodide in a solution.

Keywords: thiamacrocycle; mercury iodide; dimeric complex; exocyclic coordination; sulfoxidation

check for updates

Citation: Ju, H.; Lee, D.H.; Kim, S.; Kim, J.R.; Kang, Y.; Lee, E.; Park, I.-H. Formation of an Unusual *Pseudo*-Square Planar-Induced Mercury(II) Dimeric Complex. *Crystals* **2023**, *13*, 1475. https://doi.org/10.3390/cryst13101475

Academic Editors: Helmut Cölfen, Shujun Zhang, Jesús Sanmartín-Matalobos, Heike Lorenz and Sławomir Grabowski

Received: 8 August 2023
Revised: 3 October 2023
Accepted: 9 October 2023
Published: 10 October 2023

1. Introduction

Macrocyclic ligands play a critical role in supramolecular coordination chemistry due to their specific ability to selectively bind and self-assemble with particular metals or guest molecules [1–16]. This selectivity is the result of their unique structure, which forms a cyclic cavity that can accommodate specific species. Traditionally, the majority of macrocyclic ligands have been employed for endocyclic coordination, where the metal is located within the cavity. However, there is a sulfur-containing macrocycle known as thiamacrocycle that exhibits a preference for exocyclic coordination, meaning the metal binds to the exterior of the cavity rather than being encapsulated inside it [4]. This preference arises from the positioning of sulfur atoms, which tend to point towards the outside of the cavity [17–20]. The ability of thiamacrocycles to undergo exocyclic coordination has proven to be advantageous in creating both discrete and polymeric metallosupramolecules with unusual structures [21,22]. Discrete metallosupramolecules are distinct, well-defined entities, while polymeric metallosupramolecules form extended structures. In their previous research, the authors of this text reported on the synthesis of both discrete and network supramolecular complexes using thiamacrocycles' exo-coordination [23–28]. These complexes not only have intriguing structures but also show promise as photophysical sensors, making them attractive for potential applications in sensing and related fields.

Recently, we reported endo-coordinated metal complexes of 19-membered NO_2S_2-macrocycle (**L**) [29–31]. Encouraged by these findings, we were intrigued to expand our investigations into the creation of exo-coordinated complexes involving **L**. In this work, by using the mercury(II) iodide, we successfully synthesized exo-coordination complexes

(**1** and **2**) depending on the metalation methods. In particular, compound **2** shows an unusual *pseudo*-square planar-induced mercury(II) complex, which has Hg-$O_{sulfoxide}$ bonds formed by the oxidation of **L** to $\mathbf{HL_{ox}}$ (Scheme 1).

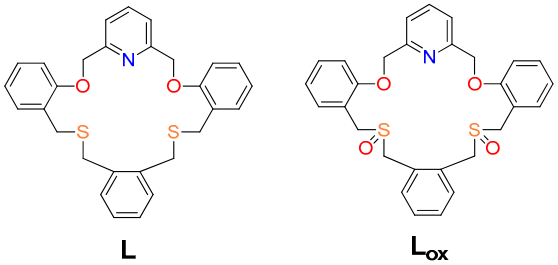

Scheme 1. (**Left**) Macrocycle ligand, **L** and (**right**) its oxidized form ($\mathbf{L_{ox}}$).

2. Experimental Details

2.1. General

All chemicals and solvents used in the syntheses were of reagent grade and were used without further purification. Elemental analyses were carried out on a LECO CHNS-932 elemental analyzer. The FT-IR spectra were recorded using a Varian 640-IR FT-IR spectrometer with KBr pellets. Thermogravimetric curves were collected in a TA Instruments TGA-Q50 thermogravimetric analyzer. Samples were heated at a constant rate of 10 °C min^{-1} from room temperature to 700 °C in a continuous-flow nitrogen atmosphere. The ESI mass spectra were obtained by using a Thermo Scientific LCQ Fleet spectrometer. NMR spectra were recorded using a Bruker DRX 300 spectrometer. The powder X-ray diffraction (PXRD) experiments were performed in a transmission mode with a Bruker GADDS diffractometer equipped with graphite-monochromated Cu Kα radiation (λ = 1.54073 Å). The crystal structure of the crystallized samples of **1** and **2** were determined by single-crystal diffraction methods at the Korea Basic Science Institute (KBSI, Western Seoul Center, Republic of Korea). All single crystals were picked up with paratone oil and mounted on a Bruker D8 Venture PHOTON III M14 diffractometer equipped with a graphite-monochromated Mo Ka (λ = 0.71073 Å) radiation source and a nitrogen cold stream (−100 °C).

2.2. Preparation of $[Hg_2(L)_2I_4]$ (**1**)

HgI_2 (28.1 mg, 0.062 mmol) in methanol (1.0 mL) was added to a solution of **L** (10.0 mg, 0.021 mmol) in dichloromethane (1.0 mL) in a vial (10 mL). Slow evaporation of the solution afforded a colorless crystalline product **1** suitable for X-ray analysis, which was obtained in the tube after 5 days. Yield: 38%. Mp: 179–182 °C. Anal. calc. for $C_{58}H_{54}Hg_2I_4N_2O_4S_4$: C, 37.05; H, 2.89; N, 1.49; S, 6.82. Found: C, 37.22; H, 2.78; N,1.53; S, 6.74%. Mass spectrum m/z (ESI): 814.15 for $[Hg(\mathbf{L})I]^+$.

2.3. Preparation of $[Hg_2(HL_{ox})I_5]_2[HgI_2]$ (**2**)

HgI_2 (28.1 mg, 0.062 mmol) in methanol (1.0 mL) was layered to diffuse slowly into a solution of **L** (10.0 mg, 0.021 mmol) in dichloromethane (1.0 mL) in a capillary tube (i.d. 5 mm). The colorless crystalline product **2** suitable for single crystal X-ray diffraction analysis was obtained in the tube after 6 months. Yield: 10%. Mp: 196–198 °C. Anal. calc. for $C_{58}H_{56}Hg_5I_{12}N_2O_8S_4$: C, 19.55; H, 1.58; N, 0.79; S, 3.60 Found: C, 19.36; H, 1.53; N, 0.83; S, 3.38%. Mass spectrum m/z (ESI): 846.19 for $[Hg(\mathbf{L_{ox}})I]^+$.

2.4. X-ray Crystallographic Analysis

Data collection, integration, and crystal size measurement were performed with SMART APEX3 (Bruker, 2016) and SAINT (Bruker, 2016) [32,33]. The absorption correction was performed by a multi-scan method implemented in SADABS [32]. The structure was solved by direct methods and refined by full-matrix least-squares on F^2 using SHELXTL with ShelXle [34]. All the non-hydrogen atoms were refined anisotropically, and the

hydrogen atoms were added to their geometrically ideal positions. Relevant crystal data collection and refinement data for the crystal structures are summarized in Table 1.

Table 1. Crystal and Experimental Data and Refinement Parameters of **1** and **2**.

	1	**2**
Formula	$C_{58}H_{54}Hg_2I_4N_2O_4S_4$	$C_{58}H_{56}Hg_5I_{12}N_2O_8S_4$
Formula weight	1880.05	3563.03
Temperature (K)	173(2)	173(2)
Crystal system	Triclinic	Triclinic
Space group	*P*-1	*P*-1
Z	1	1
a (Å)	10.8122(2)	9.8757(4)
b (Å)	12.4339(3)	12.2733(5)
c (Å)	12.5499(3)	17.2275(7)
α (°)	107.122(1)	98.794(2)
β (°)	109.305(1)	96.499(2)
γ (°)	99.581(1)	93.098(2)
V (Å^3)	1455.21(6)	2044.87(14)
D_{calc} (g/cm^3)	2.145	2.893
$2\theta_{max}$ (°)	52.00	52.00
R_1, wR_2 [$I > 2\sigma(I)$]	0.0317, 0.0648	0.0717, 0.2302
R_1, wR_2 [all data]	0.0357, 0.0669	0.0998, 0.2538
Goodness-of-fit on F^2	1.078	1.060
Independent reflections	5737 [R_{int} = 0.0329]	7934 [R_{int} = 0.0337]
Reflections collected	24044	30574

CCDC 2282620-2282621 contains the supplementary crystallographic data for this paper. These data can be obtained free of charge via http://www.ccdc.cam.ac.uk/conts/retrieving.html (accessed on 23 July 2023) (or from the CCDC, 12 Union Road, Cambridge CB2 1EZ, UK; Fax: +44 1223 336033; E-mail: deposit@ccdc.cam.ac.uk).

3. Results and Discussion

3.1. Structural Description of the Mercury(II) Complex **1**

First, a colorless crystalline product **1** was obtained by slowly evaporating a mixed solution of **L** and HgI_2 in dichloromethane/methanol. Crystal **1** crystallizes in the triclinic space group *P*-1 with the formula [$(Hg_2I_4)\mathbf{L}_2$] and adopts a 2:2 dimeric complex (Figures 1 and S1, see in Supplementary Materials). The asymmetric unit of **1** contains one ligand, one mercury atom, and two iodide ions. The cyclic dimeric structure is formed through an inversion center. The mercury(II) center is four-coordinated, being bound to two bridging sulfur atoms in **L** and two iodide atoms. The coordination geometry of Hg(II) can be described as a see-saw (saw-horse) geometry (Figure S3 and Table S1). In **1**, the bond distances of Hg–S (Hg1-S1 is 2.8014(13) Å and Hg1-S2A is 3.0054(13) Å) are longer than the normal range of Hg–S (2.5–2.8 Å), which is less than the sum of the van der Waals radii of 3.53 Å (Hg = 1.73, S = 1.80 Å) [35]. Meanwhile, the bond distances of Hg–I (av. 2.634 Å) are within the normal range.

3.2. Structural Description of the Mercury(II) Complex **2**

A dichloromethane solution for **L** was allowed to diffuse slowly to a methanol solution of HgI_2 in a capillary tube (i.d. 5 mm). The colorless crystalline product **2** was obtained in the tube after 6 months. Crystal **2** crystallizes in the triclinic space group *P*-1 with the formula $[Hg_2(\mathbf{HL_{ox}})I_5]_2[HgI_2]$, composed of two exo-coordinated Hg(II) complexes $[Hg_2(\mathbf{HL_{ox}})I_5]_2$ and a linear [I-Hg-I] metal cluster (Figures 2a and S2). The asymmetric unit of **2** contains one $\mathbf{L_{ox}}$, two and half Hg atoms and six iodide anions. Surprisingly, **L** was oxidized in the disulfoxide form ($\mathbf{HL_{ox}}$) in this condition. In particular, a hydrogen atom was added to the nitrogen atom by charge balance. It is relevant to the above

that we have previously reported the air-oxidation of sulfur donors to disulfoxides in the macrocyclic ligands. [26,36] Due to these past examples, we conclude that $\mathbf{HL_{ox}}$ was generated by air-oxidation.

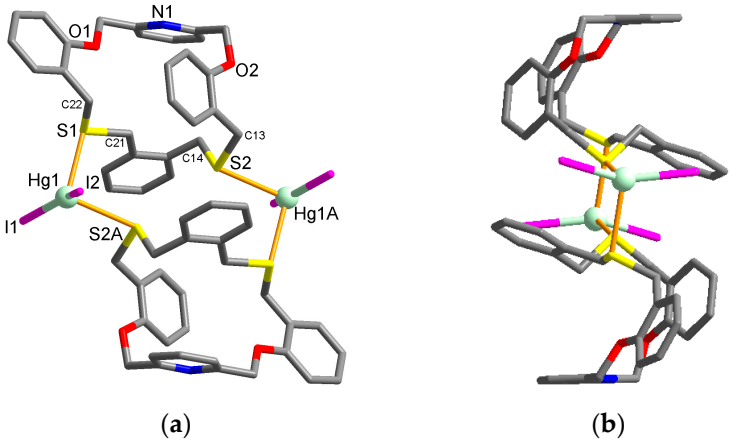

Figure 1. Mercury(II) iodide cyclic dimer complex $[(Hg_2I_4)\mathbf{L}_2]$ (**1**): (**a**) general and (**b**) side view.

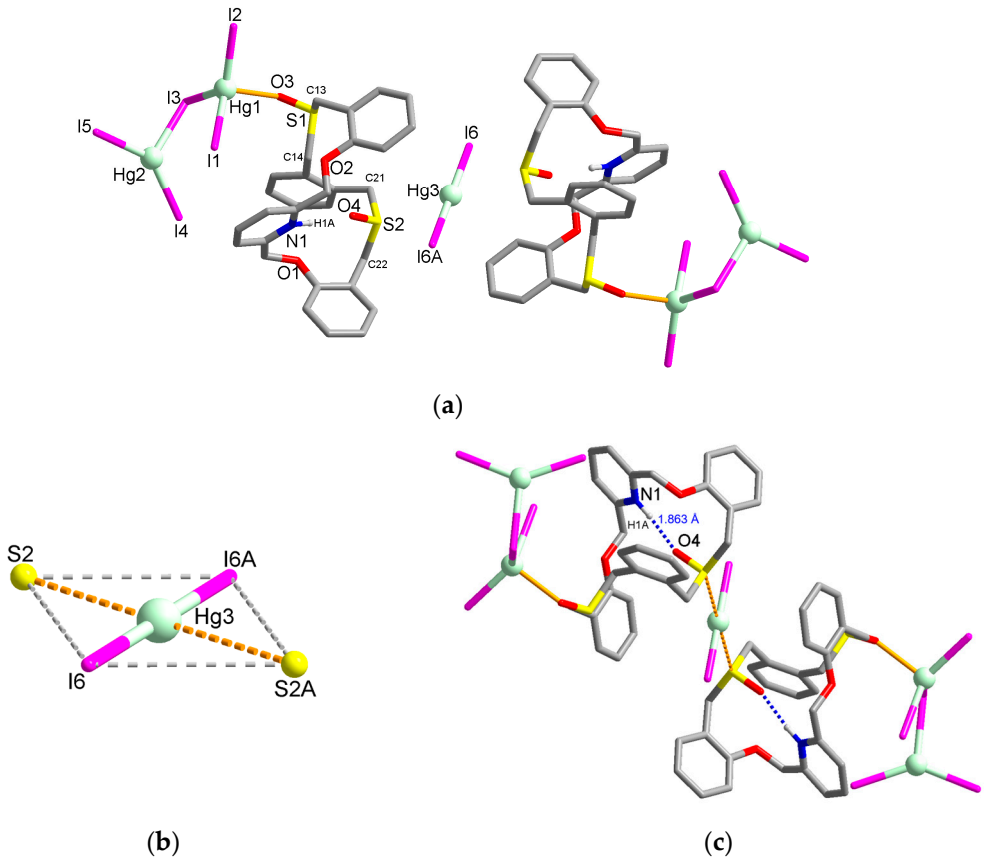

Figure 2. Crystal structure of **2**, $[Hg_2(H\mathbf{L_{ox}})I_5]_2[HgI_2]$: (**a**) view of the three-separated parts, (**b**) the *pseudo*-square planar geometry of the Hg(II) center in the metal cluster unit [∠I6−Hg3−I6A 180.0°] and (**c**) the intermolecular interaction between the pyridine ring and sulfoxide t[N1-H1A···O4 (blue dashed lines): 1.863 Å; N1···O4 2.699 Å].

In the mercury(II) complex part, there are two crystallographically independent Hg(II) atoms (Hg1 and Hg2). The Hg1 atom has a four-coordinated tetrahedral structure with three iodine ions and one sulfoxide oxygen atom (O3) from $\mathbf{HL_{ox}}$ [Hg1-O3 2.499(11) Å]. Meanwhile, the Hg2 ion has a three-coordinated structure with three iodine ions [av. Hg2-I

2.715 Å]. The coordination geometry of the Hg2 atom can be described as a distorted trigonal planar geometry (105.97(5)-139.92(5)°).

The linear (I^-–Hg^{2+}–I^-) metal cluster in **2** is located between the two Hg(II) complexes. The metal cluster has a weak interaction with the adjacent Hg(II) complexes, resulting in a *pseudo*-square planar geometry [S2-Hg3-S2A 180°] (Figure 2b). The distance between the Hg3 atom and the S2 atoms in **2** is 3.553 Å, which although being less than the sum of van der Waals radii of both ions is much higher than the usual bond length [35]. The interaction of Hg3 and S2 atoms forms an unusual *pseudo*-square planar-induced mercury(II) complex (Figure S4 and Table S2).

Besides the sulfoxidation of the ligand of **2**, the ligand $\mathbf{L_{ox}}$ was protonated rather than neutral, resulting in the formation of hydrogen on the pyridine. The hydrogen stabilizes the structure by hydrogen bonding with intramolecular sulfoxide oxygen. Due to the intramolecular interaction, the distance between O4 and H1A is 1.863 Å, slightly shorter than the general distance (Figure 2c) (the angle of C13-S1-C14 is 95.49° and the angle of C21-S2-C22 is 101.61°). As a result, the sulfoxide O4 has some difficulties in the formation of coordination bonds between Hg1.

The documented sulfoxidation of **L** upon its complexation with mercury(II) iodide was further validated through an IR study (Figure 3). In the IR spectrum of **2**, a distinct peak at 1006 cm^{-1} was identified and attributed to the stretching mode (νS=O) of the sulfoxide group.

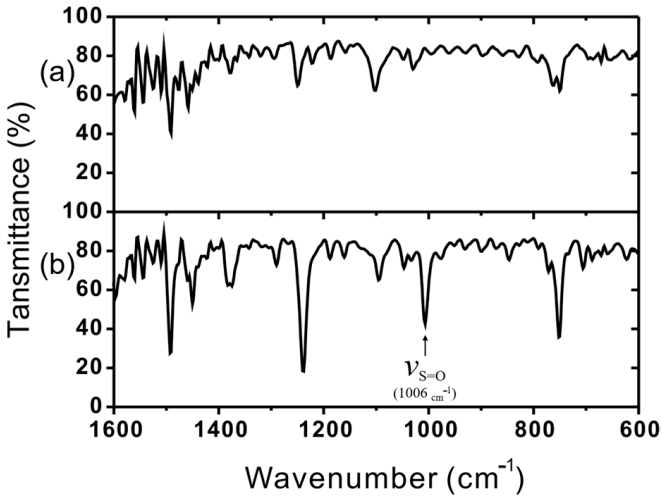

Figure 3. IR spectra of (**a**) **L** and (**b**) **2**.

3.3. Thermal Stability of **1** *and* **2**

TGA experiments were conducted to explore the thermal stability of compounds **1** and **2**, as shown in Figures S7 and S8. The samples were subjected to gradual heating at a consistent pace of 10 °C per minute, starting from ambient temperature and progressing up to 700 °C, all within an uninterrupted flow of nitrogen gas. The TGA curves unveiled a slight disparity in the thermal stability between **1** and **2**. The TGA profiles for both complexes **1** and **2** demonstrate that there is no degradation of organic ligand molecules until temperatures reach 215 °C and 210 °C, respectively, consistent with the tight, well-packed solid-state structures. Upon further elevating the temperature to approximately 400 °C, decomposition of the complexes ensued.

3.4. Solution Study of the Complexation by NMR Titration

A ^{1}H NMR titration experiment was conducted to gain further insights into the complexation behavior of **L** in a solution state with HgI_2. The experiment was performed in a mixture of $CDCl_3/CD_3OD$ (1:1), as shown in Figure 4. As HgI_2 (ranging from 0 to 3.0 equiv.) was incrementally introduced to **L**, the signals corresponding to aliphatic

protons (H_2 and H_3) experienced a downfield shift, indicating rapid ligand exchange on the NMR time scale (Figure 4c). Notably, the downfield shifts for H_2 and H_3, which are adjacent to the S donor, can be attributed to the strong binding of mercury(II) to the S donors. Conversely, the lack of change for H_1, located near the O donor, suggests no significant contribution of the O donors to the coordination with the mercury(II) center. These findings affirm that the mercury(II) ion is primarily stabilized by the sulfur donors, and the involvement of the −O−NPy−O− segment is minimal, aligning with the observations in the solid state. The titration curves reveal a multi-step complexation process, yielding two or more coexisting species depending on the mole ratio. This is a consequence of the sulfur donors' ability to interact with multiple mercury(II) ions as the concentration of mercury(II) increases.

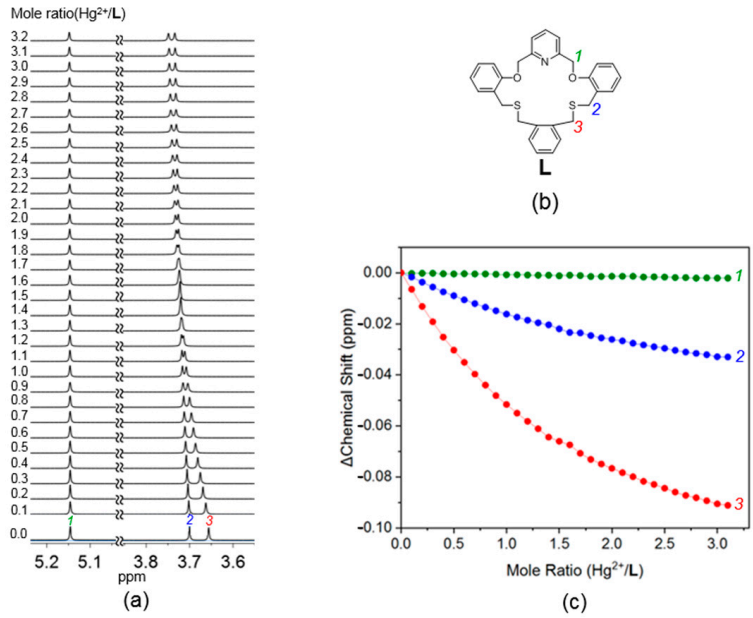

Figure 4. (**a**) ^{1}H NMR titration of **L** (1.0×10^{-2} M) with mercury(II) iodide in $CDCl_3/CD_3OD$ (v/v 1:1), (**b**) **L** and (**c**) titration curves for each proton in **L**.

4. Conclusions

In summary, we report the assembly and structural characterization of supramolecular mercury(II) iodide complexes with 19-membered macrocycle (**L**) and the disulfoxide form (**HL$_{ox}$**). Depending on the metalation conditions (slow evaporation and slow diffusion) with HgI_2, two exo-coordinated complexes, which show different topologies and stoichiometries, were obtained. In particular, the slow diffusion method in the capillary tube gave an unusual mercury(II) complex which shows three-separated parts (two exo-coordinated complexes and a metal cluster). Also, **L** was oxidized in the disulfoxide form (**HL$_{ox}$**) in this condition. The results demonstrate that different crystallization methods can be utilized for the fabrication of emerging varieties of macrocyclic complexes with different topologies. The significance of macrocycles in supramolecular chemistry lies in their ability to generate large cyclic structures. The macrocycles hold a pivotal position in the realm of supramolecular chemistry due to their unique and diverse properties such as selective binding, host–guest chemistry, self-assembly, molecular machines, catalysis, drug design, and so forth. We believe that because the study of giant rings in supramolecular chemistry opens up exciting avenues for creating sophisticated functional materials, understanding molecular recognition processes, and developing innovative technologies across various scientific disciplines. Currently, an ongoing study is being conducted to explore these and related systems further, along with their potential applications.

Supplementary Materials: The following supporting information can be downloaded at: https://www.mdpi.com/article/10.3390/cryst13101475/s1, Figure S1. Thermal ellipsoid plot (50% probability) of **1**; **Figure S2**. Thermal ellipsoid plot (50% probability) of **2**; Figure S3. Packing structure of **1**, $[(Hg_2I_4)L_2]$ along (a) a-axis, (b) b-axis and (c) c-axis; Figure S4. Packing structure of **2**, $[Hg_2(HL_{ox})I_5]_2[HgI_2]$ along (a) a-axis, (b) b-axis and (c) c-axis; Figure S5. PXRD patterns for **1**; Figure S6. PXRD patterns for **2**; Figure S7. TGA curve of **1**; Figure S8. TGA curve of **2**; Figure S9. $_1$H NMR spectra of (a) **L** and (b) **1**; Table S1. Selected bond lengths (Å) and bond angles (°) for **1**; Table S2. Selected bond lengths (Å) and bond angles (°) for **2**.

Author Contributions: Conceptualization, Y.K. and I.-H.P.; methodology, H.J., D.H.L. and E.L.; validation, D.H.L., S.K. and Y.K.; formal analysis, H.J., S.K. and Y.K.; investigation, H.J. and J.R.K.; resources, I.-H.P.; data curation, D.H.L., S.K., Y.K. and J.R.K.; writing—original draft preparation, H.J., D.H.L., E.L. and I.-H.P.; writing—review and editing, H.J., J.R.K., E.L. and I.-H.P.; visualization, J.R.K. and E.L.; supervision, I.-H.P.; project administration, E.L. and I.-H.P.; funding acquisition, E.L. and I.-H.P. All authors have read and agreed to the published version of the manuscript.

Funding: This research was funded by the NRF of Korea (2021R1C1C1006765, 2021R1C1C1009657, and 2022R1A4A1022252) and COMPA (2023-23020001-11, R&D Equipment Engineer Education Program). H. Ju acknowledges financial support from the Korea Basic Science Institute (KBSI) grant (C317000).

Institutional Review Board Statement: Not applicable.

Informed Consent Statement: Not applicable.

Data Availability Statement: The data presented in this study are available in Supplementary Materials.

Conflicts of Interest: The authors declare no conflict of interest.

References

1. Pedersen, C.J. Cyclic Polyethers and Their Complexes with Metal Salts. *J. Am. Chem. Soc.* **1967**, *89*, 2495–2496. [CrossRef]
2. Lindoy, L.F. *The Chemistry of Macrocyclic Ligand Complexes*; Cambridge University Press: Cambridge, UK, 1989.
3. Lehn, J.-M. *Supramolecular Chemistry, Concept and Perspectives*; VCH: Weinheim, Germany, 1995.
4. Lindoy, L.F.; Park, K.-M.; Lee, S.S. Metals, macrocycles and molecular assemblies—Macrocyclic complexes in metallo-supramolecular chemistry. *Chem. Soc. Rev.* **2013**, *42*, 1713–1727. [CrossRef] [PubMed]
5. Christensen, J.J.; Eatough, D.J.; Izatt, R.M. The Synthesis and Ion Bindings of Synthetic Multidentate Macrocyclic Compounds. *Chem. Rev.* **1974**, *74*, 351–384. [CrossRef] [PubMed]
6. Alexander, V. Design and Synthesis of Macrocyclic Ligands and Their Complexes of Lanthanides and Actinides. *Chem. Rev.* **1995**, *95*, 273–342. [CrossRef]
7. Jia, S.; Zhu, X.; Yin, B.; Dong, Y.; Sun, A.; Li, D. Macrocyclic Hexagonal Bipyramidal Dy(III)-Based Single-Molecule Magnets with a D6h Symmetry. *Cryst. Growth Des.* **2023**, *23*, 6967–6973. [CrossRef]
8. Li, Y.; Wang, N.; Lei, H.; Li, X.; Zheng, H.; Wang, H.; Zhang, W.; Cao, R. Bioinspired N4-metallomacrocycles for electrocatalytic oxygen reduction reaction. *Coord. Chem. Rev.* **2021**, *442*, 213996. [CrossRef]
9. Yudin, A.K. Introduction: Macrocycles. *Chem. Rev.* **2019**, *119*, 9723. [CrossRef]
10. Chen, J.-F.; Ding, J.-D.; Wei, T.-B. Pillararenes: Fascinating planar chiral macrocyclic arenes. *Chem. Commun.* **2021**, *57*, 9029–9039. [CrossRef]
11. Fang, Y.; Deng, Y.; Dehaen, W. Tailoring pillararene-based receptors for specific metal ion binding: From recognition to supramolecular assembly. *Coord. Chem. Rev.* **2020**, *415*, 213313. [CrossRef]
12. Matazova, E.V.; Egorova, B.V.; Zubenko, A.D.; Pashanova, A.V.; Mitrofanov, A.A.; Fedorova, O.A.; Ermolaev, S.V.; Vasiliev, A.N.; Kalmykov, S.N. Insights into Actinium Complexes with Tetraacetates—AcBATA versus AcDOTA: Thermodynamic, Structural, and Labeling Properties. *Inorg. Chem.* **2023**, *62*, 12223–12236. [CrossRef]
13. Hastings, C.D.; Huffman, L.S.X.; Tiwari, C.K.; Betancourth, J.G.; Brennessel, W.W.; Barnett, B.R. Coordinatively Unsaturated Metallates of Cobalt(II), Nickel(II), and Zinc(II) Guarded by a Rigid and Narrow Void. *Inorg. Chem.* **2023**, *62*, 11920–11931. [CrossRef] [PubMed]
14. Dopp, C.M.; Golwankar, R.R.; Kelsey, S.R.; Douglas, J.T.; Erickson, A.N.; Oliver, A.G.; Day, C.S.; Day, V.W.; Blakemore, J.D. Vanadyl as a Spectroscopic Probe of Tunable Ligand Donor Strength in Bimetallic Complexes. *Inorg. Chem.* **2023**, *62*, 9827–9843. [CrossRef] [PubMed]
15. Xia, Z.-J.; Zhong, Y.-M.; Hu, S.-J.; Cai, L.-X.; Sun, Q.-F. Dynamic Interconversion and Induced-Fit Guest Binding with Two Macrocycle-Based Coordination Cages. *Inorg. Chem.* **2023**, *62*, 8293–8299. [CrossRef] [PubMed]

16. Ghanbari, B.; Asadi Mofarrah, L.; Clegg, J.K. Selective Supramolecular Recognition of Nitroaromatics by a Fluorescent Metal–Organic Cage Based on a Pyridine-Decorated Dibenzodiaza-Crown Macrocyclic Co(II) Complex. *Inorg. Chem.* **2023**, *62*, 7434–7445. [CrossRef]
17. Park, S.; Lee, S.Y.; Park, K.-M.; Lee, S.S. Supramolecular Networking of Macrocycles Based on Exo-Coordination: From Discrete to Continuous Frameworks. *Acc. Chem. Res.* **2012**, *45*, 391–403. [CrossRef]
18. Wolf, R.E., Jr.; Hartman, J.R.; Storey, J.M.E.; Foxman, B.M.; Cooper, S.R. Crown thioether chemistry: Structural and conformational studies of tetrathia-12-crown-4, pentathia-15-crown-5, and hexathia-18-crown-6. Implications for ligand design. *J. Am. Chem. Soc.* **1987**, *109*, 4328–4335. [CrossRef]
19. Thomsen, D.S.; Schiøtt, B.; Jørgensen, K.A. Regioselective monoepoxidation of 1,3-dienes catalysed by transition-metal complexes. *J. Chem. Soc. Chem. Commun.* **1992**, 1072–1074. [CrossRef]
20. RajanBabu, T.V.; Nugent, W.A.; Taber, D.F.; Fagan, P.J. Stereoselective cyclization of enynes mediated by metallocene reagents. *J. Am. Chem. Soc.* **1988**, *110*, 7128–7135. [CrossRef]
21. Sato, M.; Anano, H. The transition-metal complexes of the thiamacrocycle containing two ferrocene nuclei in the main chain. Synthesis, properties, and molecular structure of Ag(I), Cu(I), Pd(II), and Pt(II) complexes of 1,5,16,21-tetrathia[5.5]ferrocenophane. *J. Organomet. Chem.* **1998**, *555*, 167–175. [CrossRef]
22. Ashton, P.R.; Burns, A.L.; Claessens, C.G.; Shimizu, G.K.H.; Small, K.; Fraser Stoddart, J.; White, A.J.P.; Williams, D.J. Thiamacrocyclic chemistry: Synthesis of a novel oxadithiacrown and its copper iodide complex. *J. Chem. Soc. Dalton Trans.* **1997**, *9*, 1493–1496. [CrossRef]
23. Lee, E.; Lee, S.G.; Park, I.-H.; Kim, S.; Ju, H.; Jung, J.H.; Ikeda, M.; Habata, Y.; Lee, S.S. Endo- and Exocyclic Coordination of a 20-Membered N2O2S2-Macrocycle and Cascade Complexation of a 40-Membered N4O4S4-Macrocycle. *Inorg. Chem.* **2018**, *57*, 6289–6299. [CrossRef] [PubMed]
24. Lee, H.-H.; Lee, E.; Ju, H.; Kim, S.; Park, I.-H.; Lee, S.S. Influence of Anion and Mole Ratio on the Coordination Behavior of an NO2S3-Macrocycle: The Formation of a Dumbbell-Shaped Macrocyclic Cadmium(II) Iodide Complex. *Inorg. Chem.* **2016**, *55*, 2634–2640. [CrossRef] [PubMed]
25. Shin, M.; Ju, H.; Habata, Y.; Lee, S.S. Coordination behaviors of a 23-membered NO_4S_2-macrocycle: Mononuclear silver(I) complex and conformational isomers of tetranuclear bis(macrocycle) mercury(II) complexes exhibiting exo- and endo/exocyclic coordination modes. *Inorg. Chim. Acta* **2018**, *482*, 749–755. [CrossRef]
26. Kim, S.; Park, I.-H.; Choi, H.B.; Ju, H.; Lee, E.; Herng, T.S.; Ding, J.; Jung, J.H.; Lee, S.S. Formation of a four-bladed waterwheel-type chloro-bridged dicopper(ii) complex with dithiamacrocycle via double exo-coordination. *Dalton Trans.* **2020**, *49*, 1365–1369. [CrossRef]
27. Seo, S.; Lee, E.; Ju, H.; Kim, S.; Park, I.-H.; Jung, J.H.; Lee, S.S. Influence of mole-ratio on the coordination behaviour of a ditopic $N_2O_2S_2$-macrocycle: Endo/exocyclic silver(i) coordination polymer exhibiting desolvation-induced SCSC transformation. *CrystEngComm* **2017**, *19*, 7185–7190. [CrossRef]
28. Kim, S.; Siewe, A.D.; Lee, E.; Ju, H.; Park, I.-H.; Park, K.M.; Ikeda, M.; Habata, Y.; Lee, S.S. Ligand-Induced Formation of Copper(I) Iodide Clusters: Exocyclic Coordination Polymers with Bis-dithiamacrocycle Isomers. *Inorg. Chem.* **2016**, *55*, 2018–2022. [CrossRef]
29. Kang, Y.; Park, I.-H.; Ikeda, M.; Habata, Y.; Lee, S.S. A double decker type complex: Copper(i) iodide complexation with mixed donor macrocycles via [1:1] and [2:2] cyclisations. *Dalton Trans.* **2016**, *45*, 4528–4533. [CrossRef]
30. Kang, Y.; Lee, H.-H.; Ju, H.; Lee, E.; Kim, S.; Lee, J.-H.; Park, I.-H.; Lee, S.S. Endocyclic and Endo–Exocyclic Silver(I) Complexes of Thiaoxaaza Macrocycles: Crystallographic and NMR Studies. *Aust. J. Chem.* **2017**, *70*, 456. [CrossRef]
31. Park, I.-H.; Kang, Y.; Lee, E.; Ju, H.; Kim, S.; Seo, S.; Jung, J.H.; Lee, S.S. Snapshot and crystallographic observations of kinetic and thermodynamic products for NO_2S_2 macrocyclic complexes. *IUCrJ* **2018**, *5*, 45–53. [CrossRef]
32. Bruker, A.I.; Madison, W. *USA, SMART, SAINT and SADABS*; Bruker AXS Inc.: Billerica, MA, USA, 2016.
33. Sheldrick, G.M. *SADABS*; Version 2.03; University of Göttingen: Göttingen, Germany, 2002; pp. 1600–5368.
34. Bruker, A.I.; Madison, W. *SHELXTL*; Version 6.10; Bruker AXS, Inc.: Billerica, MA, USA, 2000.
35. Bondi, A. van der Waals Volumes and Radii. *J. Phys. Chem.* **1964**, *68*, 441–451. [CrossRef]
36. Park, I.-H.; Lee, S.S. Networking of macrocycles: 1D and 2D coordination polymers of dithia-18-crown-6 with copper(ii) and copper(i). *CrystEngComm* **2011**, *13*, 6520. [CrossRef]